

# Optical inhibition of striatal neurons promotes focal neurogenesis and neurobehavioral recovery in mice after middle cerebral artery occlusion

Xiaosong He<sup>1,2,\*</sup>, Yifan Lu<sup>2,\*</sup>, Xiaojie Lin<sup>2</sup>, Lu Jiang<sup>2</sup>,  
Yaohui Tang<sup>2</sup>, Guanghui Tang<sup>2</sup>, Xiaoyan Chen<sup>2</sup>, Zhijun Zhang<sup>2</sup>,  
Yongting Wang<sup>2,3</sup> and Guo-Yuan Yang<sup>2,4</sup>

## Abstract

Striatal neurons regulate the activity of neural progenitor cells in the subventricular zone, but the effect of striatal neuronal activity on neurogenesis after ischemic stroke is unclear. In this study, we used optogenetic tools to investigate the impact of striatal neuronal activity on the neurogenesis and functional recovery after cerebral ischemia. We transfected striatal neurons with channelrhodopsin-2 or halorhodopsin from *Natronomonas* so that they can be excited by 473 nm laser or inhibited by 594 nm laser, respectively. Neural inhibition but not excitation at 4–7 days after middle cerebral artery occlusion resulted in reduced atrophy volume ( $6.8 \pm 0.7$  vs  $8.5 \pm 1.2$  mm<sup>3</sup>,  $p < 0.05$ ) and better performance represented by longer sustaining time on rotarod ( $99.3 \pm 9$  vs  $80.1 \pm 11$  s,  $p < 0.01$ ) and faster moving speed ( $7.7 \pm 2$  vs  $5.7 \pm 1.1$  cm/s,  $p < 0.05$ ) in open field tests. Furthermore, neural inhibition increased the number of nestin<sup>+</sup>, BrdU<sup>+</sup>/doublecortin<sup>+</sup> and BrdU<sup>+</sup>/NeuN<sup>+</sup> cells ( $p < 0.001$ ) in the subventricular zone and peri-focal region, and the expression level of axon guidance factor Netrin-1 ( $0.39 \pm 0.16$  vs  $0.16 \pm 0.02$ ,  $p < 0.05$ ) in the peri-focal region. These data suggest that striatal neuronal activity plays an important role in regulating neurogenesis and neural-behavioral outcomes, and that inhibiting striatal neurons by optogenetics promotes the recovery after ischemic stroke in mice.

## Keywords

Brain ischemia, neurogenesis, optogenetics, striatal neurons, Netrin-1

Received 8 November 2015; Accepted 8 March 2016

## Introduction

Neurogenesis refers to the proliferation, differentiation, migration and integration of neural stem cells both at the physiological or pathological conditions.<sup>1</sup> In the subventricular zone (SVZ), nestin or glial fibrillary acidic protein (GFAP) positive neural stem cells (NSCs) give rise to transiently amplified cells. These transiently amplified cells further develop into immature neurons named neuroblasts.<sup>2</sup> Under physiological condition, immature neurons from the SVZ can migrate to the olfactory bulb through the rostra migratory stream and differentiate into GABAergic interneurons, which can integrate into the local network and contribute to olfactory functions.<sup>3</sup> After brain ischemia, the neural stem cells in the SVZ exit from quiescence and start to proliferate. The resulting neuroblasts migrate to

<sup>1</sup>Department of Human Anatomy, Guangzhou Medical University, Guangzhou, China

<sup>2</sup>Neuroscience and Neuroengineering Research Center, Med-X Research Institute and School of Biomedical Engineering, Shanghai Jiao Tong University, Shanghai, China

<sup>3</sup>Brain Science and Technology Research Center, Shanghai Jiao Tong University, Shanghai, China

<sup>4</sup>Shanghai Ruijin Hospital, School of Medicine, Shanghai Jiao Tong University, Shanghai, China

\*These authors contributed equally to this work

## Corresponding author:

Guo-Yuan Yang and Yongting Wang, Neuroscience and Neuroengineering Research Center Med-X Research Institute and School of Biomedical Engineering, Shanghai Jiao Tong University, 1954 Hua Shan Road, Shanghai 200030, China.

Emails: gyyang0626@gmail.com, ytwang@sjtu.edu.cn

the boundaries of the infarct zone, differentiate into mature neurons and integrate into the neuronal network.<sup>4</sup> A number of studies have demonstrated that spontaneous neurogenesis<sup>5</sup> or neurogenesis induced by stem cell therapy and gene therapy could promote the functional recovery after ischemic stroke.<sup>6</sup>

Neuronal activity is a major factor that influences neural plasticity and the outcomes of ischemic stroke.<sup>7</sup> Enhanced excitability or reduced inhibition in cortical neurons promotes functional recovery after brain ischemia, which may involve the striatum-related neural circuits in motor function.<sup>8</sup> In addition, enhanced neuronal activity in the cortex also improves cerebral blood flow and the neurovascular coupling response, as well as the release of neural trophic factors.<sup>9</sup> Direct electrical stimulation of the striatum has a beneficial effect on the outcomes of ischemic stroke, suggesting that the change of striatal neuronal activity can influence the outcome of brain ischemia.<sup>10</sup> Moreover, neuronal activity also regulates neurogenesis. Optogenetics technique allows the modulation of specific types of neurons.<sup>11,12</sup> Using this technique, Song and colleagues<sup>13</sup> reported that parvalbumin positive interneurons are involved in local neuronal circuitry in the adult mouse hippocampus and has a direct impact on the maintenance and proliferation of NSCs. Recently, it was reported that striatal neurons project dendrites and axons into the SVZ and can induce calcium influx in neural progenitor cells.<sup>14</sup> However, it is unclear whether changing the activity of striatal neurons would promote or inhibit the neurogenesis in the SVZ after ischemic stroke.

Accompanying the reduction of the number of neurons in the striatum after brain ischemia is the increase of endogenous Netrin-1 (NT-1), which functions more than an axon guidance cue in the repair process after brain injury.<sup>15</sup> NT-1 protein injection or over-expression in the striatum was shown to be beneficial for the recovery after ischemic stroke through attenuating cell apoptosis and improving oligodendrogenesis and angiogenesis.<sup>16–18</sup> More recently, it was reported that neuronal activity plays a central role in regulating the expression of NT-1 receptor DCC.<sup>19</sup> However, whether neuronal activity regulates NT-1 expression is still unknown. In this study, we regulated striatal neuronal activity through optogenetics to investigate whether the changes in striatal neuronal activity could influence NT-1 expression, neurogenesis and the recovery after ischemic stroke.

## Methods and materials

### Animals

The ARRIVE guidelines were followed in the design and report of the current study. All procedures were

approved by the Institutional Animal Care and Use Committee of Shanghai Jiao Tong University, Shanghai, China. During the animal studies, guidelines of the regulation for the administration of affairs concerning experimental animals of China enacted in 1988 were followed. Mice were housed under standard laboratory conditions. A total of 72 adult male CD-1 mice were used in this study, 60 mice weighing 25 to 30 grams aged 4–5 weeks were randomly divided into three groups: (1) Green fluorescent (GFP) gene transfected control group, (2) ChR2-YFP gene transfected group and (3) halorhodopsin from *Natronomonas*-yellow fluorescent protein (NpHR-YFP) gene transfected group; these mice underwent gene transfer, *in vivo* electrophysiology test, MCAO surgery and laser stimulation. Another 12 mice were randomly divided into four groups to quantify the NT-1 expression after MCAO. The schedule of the experiment designed is shown in Figure 1.

### Lentivirus packaging and injection

Lentiviruses were packaged and purified as reported by Boyden et al.<sup>20</sup> Briefly, plasmid pLenti-CaMKIIa-hChR2(H134R)-EYFP-WPRE or pLenti-CaMKIIa-eNpHR 3.0-EYFP were co-transduced together with two helper plasmids into 293T cells using calcium phosphate method. After 24 hours, culture media were switched to Ultraculture (Lonza, Basel, Switzerland). The culture media were collected at 48 and 72 hours after transfection. Lentiviruses were purified by sucrose gradient ultracentrifugation. The titer of the lentiviruses used in this study was adjusted to  $1 \times 10^9$  TU/ml after the titers were determined by measuring the transfection efficiency on 293T cells. Before injection, mice were intraperitoneally anesthetized with Ketamine/xylazine (100 mg/10 mg per kg, Sigma, San Louis, MO). The mouse head was fixed on a stereotaxic plate (RWD, Shenzhen, China). A 0.5-mm diameter burr hole was drilled by a hand-drill (Fine Science Tool, Foster City, CA). Two microliters of lentiviruses suspended in phosphate buffered saline (PBS) were injected into the left striatum (AP = -0.02 mm, ML = -2.5 mm, DV = 3 mm relative to bregma) using a mini-pump (WPI, Sarasota, FL) at 100 nl/min. After finishing injection, the needle was maintained in the brain for an additional 5 minutes before it was withdrawn.

### Animal model of transient middle cerebral artery occlusion

Two weeks after lentivirus injection, mice were intraperitoneally anesthetized with Ketamine/xylazine (100 mg/10 mg per kg). Body temperature was maintained at  $37 \pm 0.5^\circ\text{C}$  using a heating pad (RWD Life Science) with feedback control. The transient middle

cerebral artery occlusion (tMCAO) surgery was performed as previously described.<sup>21</sup> Briefly, a 6-0 suture (Covidien, Mansfield, MA) with a silicone-coated round tip was inserted from the left external carotid artery (ECA) into the internal carotid artery (ICA) to occlude the middle cerebral artery (MCA). Reperfusion was achieved by withdrawing the suture at 90 minutes after occlusion. The sham groups underwent the same surgery without a suture insertion.

### *Optrode preparation, implantation and in vivo electrophysiology*

Optrodes were prepared using a custom-made optrode mold. Eight platinum-iridium alloy microelectrodes with 35  $\mu\text{m}$  diameter (Plexon, Dallas, Texas) were arranged around an optical fiber with 200  $\mu\text{m}$  diameters and 0.22 numerical apertures (Thorlabs, Newton, NJ). The distance between two neighboring microelectrodes was 200  $\mu\text{m}$ . The optical fiber and microelectrodes were coated with polyethylene glycol leaving 0.5 mm exposed to air. The other end of each microelectrode was soldered onto separate slots of a multi-pin female header after removing the coated insulation using a brief flame. Four silver microwires with 100  $\mu\text{m}$  diameter were soldered onto the female header as ground and reference electrodes. The other end of the optical fiber was fixed onto a ceramic ferrule and polished by abrasive paper to ensure efficient optical coupling. The light transmittance of the fiber was measured by an optical power meter (Thorlabs, Newton, NJ). The resistance of each microelectrode was measured by a multimeter. The optrodes used in our study had similar light transmittance and resistance.

Optrode implantation was performed on six randomly selected mice, three from the Chr2 group and three from the NpHR group, at 3 days after tMCAO. A 1  $\times$  1-mm window was drilled on the skull of anesthetized mouse and the exposed endocranium in the window was removed. After inserting the exposed end of the optrode into mouse cortex, the polyethylene glycol coating was gradually dissolved by PBS during the optrode implantation.

The optrode was slowly implanted into left striatum of mouse (AP = -0.02 mm, ML = -2.5 mm, DV = 2 mm relative to bregma) in 30 minutes. The window was filled with biogel (FST). Dental cement was used to immobilize the outer part of the optrode.

*In vivo* electrophysiological recording was performed on the day after optrode implantation. Data were recorded by electrophysiological instrument (Plexon, Dallas, Texas) and analyzed by the software Spike 2 (Plexon, Dallas, Texas). All neural electrophysiological data were band-pass filtered. Single and multi-unit activity recording were sampled at 30 kHz and

band-pass filtered at 250 Hz to 3000 Hz. Before recording, mice were intraperitoneally anesthetized with Ketamine/xylazine (100 mg/10 mg per kg). The implanted optrode was connected to electrophysiological instrument and coupled with the end of an optical fiber patch cord which was connected to laser device (Century Laser, Shanghai). At the beginning of each recording, five minutes baseline was recorded to evaluate the stability of the electrophysiological signal, followed by 15 minutes of 473 nm pulse laser or 594 nm constant laser stimulation (the parameters are provided below). After laser stimulation, another five minutes of signal was recorded.

### *Fiber implantation and laser stimulation*

All animals except the six mice for *in vivo* electrophysiology underwent fiber implantation at 7 days before tMCAO. After mice were anesthetized, a fiber with a ceramic ferrule at the outside end was implanted into the left striatum through a small burr hole (AP = -0.02 mm, ML = -2.5 mm relative to bregma) generated with a hand drill. The distance from the tip of the fiber to the surface of skull was 3.0 mm. The ceramic ferrule was immobilized on the surface of skull by dental cement, followed by wound closure.

Laser stimulation was performed twice daily from 4 to 7 days after tMCAO. Each stimulation session lasted 15 minutes. The parameters of lasers were controlled by a waveform generator (Tektronix, Shanghai, China). For the Chr2 group, each 5-second stimulation cycle composed of 1-second stimulation phase and 4-seconds rest phase. In the stimulation phase, 473 nm laser pulses with 5 ms pulse width were administered at 20 Hz. For the NpHR group, 594 nm laser was administered constantly for 15 minutes; 1 mW output power at the tip of optical fiber was used for both lasers, as measured by optical power meter as reported.<sup>22</sup>

### *Immunohistochemistry and data quantification*

Animals were sacrificed 7 days and 35 days after tMCAO for immunohistochemistry. Mice were deep anesthetized with chloral hydrate and transcardially perfused first with normal saline and then with freshly prepared 4% paraformaldehyde in PBS. Brains were quickly removed and immersed in 4% paraformaldehyde overnight at 4°C. Brains were dehydrated in 30% sucrose solution and frozen in isopentane at -80°C before sectioned into 30  $\mu\text{m}$  brain sections. Sections were treated with 0.3% Triton-PBS for 30 minutes and blocked by 5% normal donkey serum for 60 minutes, then incubated with DARPP-32 (1:200 dilution, Abcam), NeuN (1:300 dilution, Millipore Inc., Billerica, MA), and Nestin (1:200 dilutions,

Millipore) antibodies at 4°C overnight. After thoroughly rinsing with PBS, sections were incubated with secondary antibodies for 60 minutes at room temperature. For double immunofluorescence staining, antibodies for NT-1 and NeuN were incubated together, while corresponding secondary antibodies were incubated separately.

BrdU powder (Sigma, San Louis, MO) was dissolved in saline at a concentration of 20 mg/ml. BrdU solution was injected intraperitoneally at a dose of 50 mg/kg twice a day within 30 minutes after laser stimulation. For GABA receptor inhibition, GABA<sub>A</sub> receptor inhibitor bicuculline was dissolved in 0.01 M HCl and injected intraperitoneally at a dose of 0.125 mg/kg 30 minutes before laser stimulation. For BrdU double staining, sections were treated with 2 M HCl for 30 minutes then treated twice with 0.1 M boric acid (pH=8.5) for 10 minutes each before blocking with 5% normal donkey serum for 60 minutes. Sections were then incubated with BrdU (1:200 dilution, Santa Cruz) and DCX (1:300 dilution, Santa Cruz) or BrdU and NeuN (1:200 dilution, Abcam) antibodies at 4°C overnight. After thoroughly rinsing with PBS, sections were incubated with corresponding secondary antibodies for 60 minutes at room temperature.

Photomicrographs were taken with a confocal microscope under the same conditions (Leica, Solms, Germany). Five serial sections spaced 200 µm apart (bregma -0.4 mm to 0.4 mm) were selected from each brain. In the SVZ, DCX and BrdU double-positive cells were counted. Nestin staining intensity in the SVZ was computed as mean integrated optical density (IOD) as previously described.<sup>23</sup> NeuN and BrdU double-positive cells were counted in six fields randomly selected from peri-infarction region under a ×40 objective lens.

### Behavioral tests

Open-field tests and Rotarod tests were performed at 3, 7 and 35 days after tMCAO. The baseline data were acquired at 1 day before tMCAO. Animals were trained for 20 minutes daily for 2 days before the baseline test. All tests were carried out by an investigator who was blind to the grouping.

**Open-field tests.** Mice were put into the center of a chamber (75 × 75 × 75 cm) and were allowed to move freely in the field. Before the test began, animals were given 5 minutes to adjust to the environment. The movements of the mice in the next 5 minutes were recorded using a camera. The average speed of animal movement in the chamber was calculated by the any-maze software (Stoelting, Kiel, WI).

**Rotarod tests.** The task requires the mice to balance on a rotating rod. For each time of training or test, animals were allowed a 1-minute adaptation period on the rod at rest, after which the rod was steadily accelerated to 40 revolutions per minute over 2 minutes. The time that the mouse spent on the rod was recorded. Motor test data were analyzed as mean duration on the rotarod from 3 trials.

### Western blot

Proteins used for western blot experiments were extracted from a piece of ipsilateral striatal tissue, which was isolated from a 2-mm-thick brain slice, using RIPA, PMSF and Cocktail mixture. The protein concentration was measured using BCA Protein Assay Kit (ThermoPierce, Rockford, USA). An equal amount of total protein was loaded on 10% resolving gel for electrophoresis. SDS-PAGE was performed and the proteins were transferred onto nitrocellulose membrane (Whatman, Piscataway, NJ). The membrane was blocked with 5% non-fat milk for 60 minutes at room temperature and incubated with anti-mouse NT-1 antibody (1:1000 dilutions, Abcam) and anti-β-actin antibody (1:1000 dilution, Santa Cruz) at 4°C overnight. The membrane was washed in Tris buffered saline with Tween-20 (TBST) and incubated with appropriate horseradish peroxidase-conjugated anti-rabbit or anti-goat IgG for 120 minutes at room temperature, and reacted with an enhanced ECL substrate (Pierce, Rockford, IL). The result of chemiluminescence was recorded and semi-quantified by the Quantity One imaging software (Bio-Rad, Hercules, CA).

### Atrophy volume measurement

The sections were stained with 1% cresyl violet (Sigma) for 30 minutes at room temperature. Atrophy volume was calculated by NIH Image J software. Atrophy size equaled to the total contralateral hemisphere size minus total ipsilateral hemisphere size. Atrophy volume  $V$  between two adjacent sections was calculated by the formula

$$V = 1/3 \times h(S1 + S2 + \sqrt{S1 \times S2})$$

where S1 and S2 are the atrophy areas of the upper and the lower sections, respectively. The  $h$  was the distance between the two adjacent sections. Total atrophic volume was the sum of each volume between adjacent two sections.

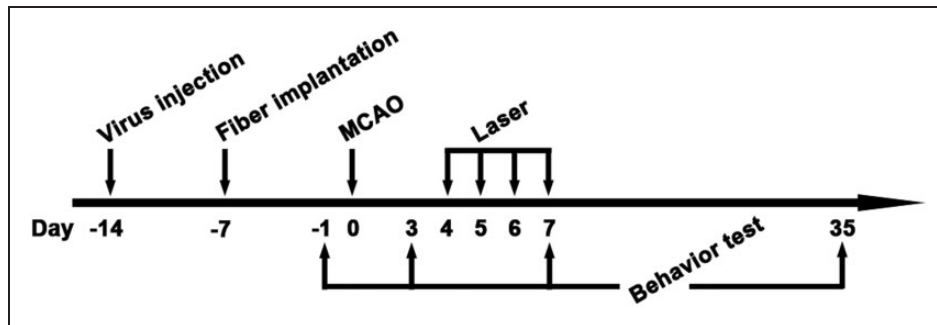


**Figure 1.** Schedule of animal experiments in this study. Lentivirus-carrying ChR2 or NpHR was injected into the striatum at 14 days before tMCAO. At 7 days before tMCAO, an optical fiber was implanted into the striatum. Animals were next trained on rotarod at 3 and 2 days before tMCAO. After tMCAO, the striatum were stimulated with 473 nm or 594 nm laser twice a day from 4 to 7 days. Open field test and Rotarod test were carried out at 1 day before tMCAO for the first time and repeated at 3, 7 and 35 days after tMCAO. Mice were sacrificed at 7 and 35 days after tMCAO for immunohistochemistry.

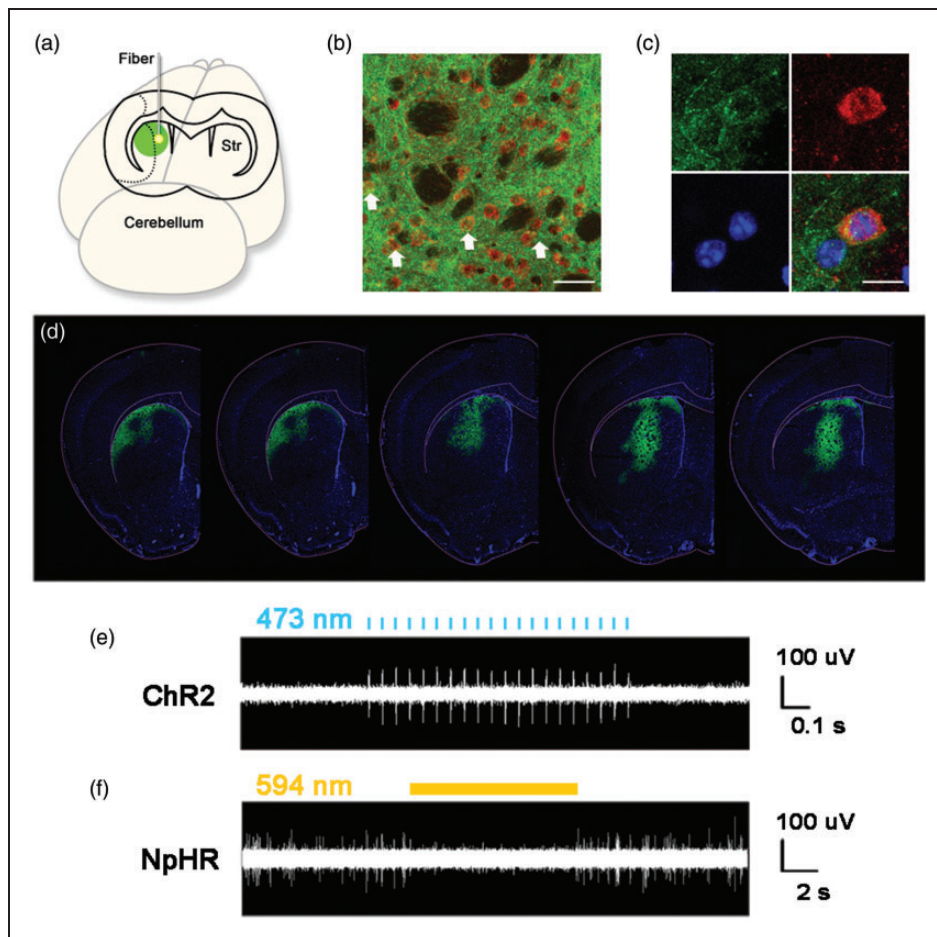


**Figure 2.** The expression of opsins in striatal neurons under CaMKII promoter and in vivo electrophysiological recording during laser stimulation. (a) The illustration of virus-mediated gene expression and laser stimulation; (b) Lentivirus-carrying opsins under the CaMKII promoter transfected striatal neurons. The white arrows show DARPP-32 and YFP double-positive medium spiny neurons. Green represents YFP-positive signals, Red represents DARPP-32-positive medium spiny neurons, Bar = 30 μm. (c) Cellular morphology of DARPP-32 and YFP double-positive neurons. Green is YFP-positive signals, Red represents DARPP-32-positive medium spiny neurons, Blue is DAPI, Bar = 30 μm. (d) YFP-positive signals in the striatum, from -0.5 mm to 0.5 mm relative to bregma. (e) The activities of striatal neurons expressing ChR2 during laser stimulation. Laser pulses of 473 nm trigger spikes in striatal neurons expressing ChR2. (f) Constant laser of 594 nm reduces the firing rate of striatal neurons expressing NpHR.

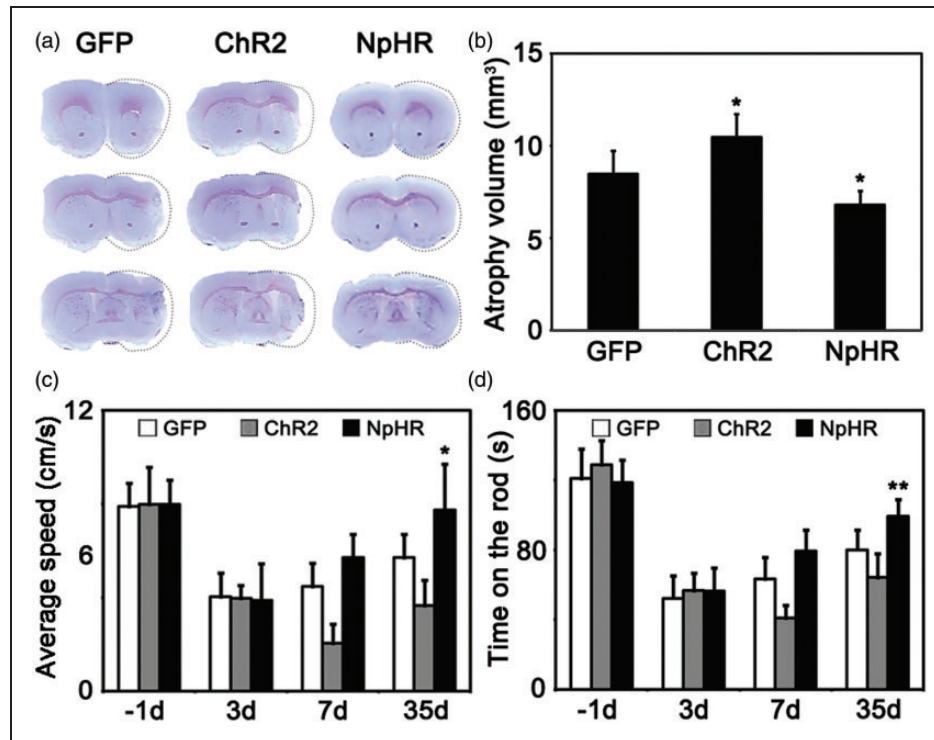


**Figure 3.** Inhibition of striatal neurons reduced the atrophy volume and promoted motor recovery after cerebral ischemia.

(a) Cresyl violet staining of brain slice at 35 days after tMCAO surgery. Dash line indicated the atrophic tissues. (b) Mice showed smaller brain atrophy volume in the inhibition group and larger atrophy volume in excitation group compared to the control. \* represents  $p < 0.05$ ,  $n = 7$ . (c) Average speed of mice in the open field test at each time point. Mice in the inhibition group moved faster compared to the control, \* represents  $p < 0.05$ ,  $n = 7$ . (d) Duration of time in Rotarod test at each time point. Mice in the inhibition group persisted for longer time on the rotating rod compared to the control, \*\* represents  $p < 0.01$ ,  $n = 7$ .

### Statistical analysis

Data were presented as mean  $\pm$  SD and analyzed by one-way ANOVA followed by Bonferroni post hoc comparison using GraphPad Prism version 3.05 (GraphPad Software, Inc., La Jolla, CA).  $p < 0.05$  was considered as statistically significant.

## Results

### Expression of opsins and verification of optogenetic stimulation in the striatal area

In the lentivirus construct, both ChR2 and NpHR genes were under the control of CaMKII promoter. Expression of these genes was tracked by a YFP gene that immediately followed these genes in the construct. Robust YFP signal was observed to be limited to the striatum at 14 days after viral injection (Figure 2(d)) and lasted for at least 2 months. The majority of the YFP-positive cells were DARPP-32-positive medium spiny neurons (Figure 2(b) and (c)). *In vivo* electrophysiology data showed that the firing rate of striatal neurons was significantly increased when stimulated with 473 nm

laser in the ChR2 group (Figure 2(e)). Striatal neuronal activity was essentially silenced by 594 nm laser stimulation in the NpHR group (Figure 2(f)). These results indicated that the activity of striatal neurons could be regulated by optogenetic method in this study.

### Inhibition of striatal neuronal activity reduced the atrophy volume and promoted recovery after tMCAO

At 35 days after tMCAO, brain atrophy measurement and behavioral tests were performed. Cresyl violet staining results showed that the total brain atrophy volume was decreased in the NpHR group compared to the control (NpHR =  $6.8 \pm 0.7 \text{ mm}^3$  vs GFP =  $8.5 \pm 1.2 \text{ mm}^3$ ,  $p < 0.05$ ,  $n = 6$ ). In contrast, brain atrophy volume increased in the ChR2 group (ChR2 =  $10.5 \pm 1.2 \text{ mm}^3$  vs GFP =  $8.5 \pm 1.2 \text{ mm}^3$ ,  $p < 0.05$ ,  $n = 6$ ) (Figure 3(a)). In the open field tests, mice in the NpHR group also displayed a faster moving speed compared to the control at 35 days after MCAO (NpHR =  $7.7 \pm 2 \text{ cm/s}$  vs GFP =  $5.7 \pm 1.1 \text{ cm/s}$ ,  $p < 0.05$ ,  $n = 7$ ) (Figure 3(b)). In addition, mice in the NpHR group maintained significantly longer time in rotarod tests compared to the control at 35 days after

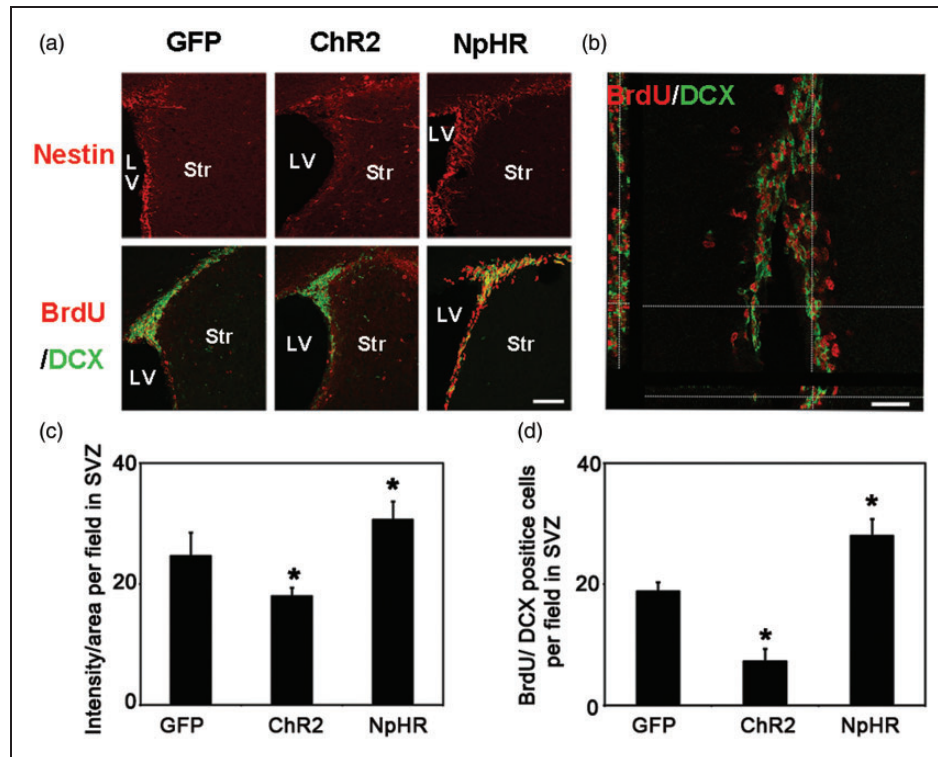


**Figure 4.** Inhibition of striatal neurons promoted neurogenesis in the SVZ after ischemic stroke. (a) Nestin-positive cells and BrdU/DCX double-positive cells in SVZ at 7 days after tMCAO, Bar = 30  $\mu$ m. (b) Three-dimensional observation of BrdU and DCX double-positive cells. Bar = 25  $\mu$ m. (c) In the SVZ, the number of nestin-positive cells increased in the inhibition group and reduced in the excitation group when compared with the control, \* represents  $p < 0.001$ ,  $n = 6$ . (d) BrdU/DCX double-positive cells in the SVZ. The number of BrdU/DCX double-positive cells in the SVZ increased in the inhibition group and reduced in the excitation group compared to the control, \* represents  $p < 0.001$ ,  $n = 6$ .

MCAO (NpHR =  $99.3 \pm 9$  s vs control =  $80.1 \pm 11$  s,  $p < 0.01$ ,  $n = 7$ ) (Figure 3(c)). These results indicated that inhibiting striatal neuronal activity promoted functional recovery after brain ischemia.

#### *Inhibition of striatal neuronal activity promoted the neurogenesis in the SVZ and peri-infarct area*

At 7 days after tMCAO, the nestin signal intensity in the SVZ was significantly increased in the NpHR group compared to the control (NpHR =  $30.6 \pm 3$  vs GFP =  $24.0 \pm 1.4$ ,  $p < 0.001$ ,  $n = 6$ ). The number of BrdU<sup>+</sup>/DCX<sup>+</sup> cells in the SVZ was significantly increased in the NpHR group (NpHR =  $56 \pm 5.5$  vs GFP =  $37.6 \pm 3$ ,  $p < 0.001$ ,  $n = 6$ ) at 7 days after tMCAO (Figure 4). In contrast, the ChR2 group showed decreased nestin intensity (ChR2 =  $18.0 \pm 1.4$  vs GFP =  $24.0 \pm 1.4$ ,  $p < 0.001$ ,  $n = 6$ ) and reduced number of BrdU<sup>+</sup>/DCX<sup>+</sup> cells (ChR2 =  $14.5 \pm 4.2$  vs GFP =  $37.6 \pm 3$ ,  $p < 0.001$ ,  $n = 6$ ) in the SVZ. At 35 days after tMCAO, in the peri-infarct region, the NpHR group had significantly higher number of BrdU<sup>+</sup>/NeuN<sup>+</sup> cells compared to the control (NpHR =  $49.9 \pm 6$  per field vs

GFP =  $37.6 \pm 3$  per field,  $p < 0.001$ ,  $n = 6$ ) (Figure 5). These results suggested that the inhibition of striatal neuronal activity promoted neural stem cell proliferation in the SVZ and the maturation of neural progenitor cells in the peri-infarct region after ischemic stroke.

#### *Changing of striatal neuronal activity influenced NT-1 expression*

Immunofluorescent staining showed that NT-1 was expressed in neurons after tMCAO (Figure 6(c)), which agreed with the results from previous studies.<sup>15</sup> In mice without light stimulation, the expression of NT-1 was increased at 3 days after tMCAO when compared to sham group (tMCAO3d =  $0.23 \pm 0.06$  vs Sham =  $0.06 \pm 0.03$ ,  $p < 0.05$ ,  $n = 3$ ) (Figure 6(a)). We further examined whether NT-1 expression could be influenced by the activity of striatal neuron after ischemic stroke. Our results showed that the expression of NT-1 was significantly higher in the NpHR group when compared to the control group (NpHR =  $0.39 \pm 0.16$  vs GFP =  $0.16 \pm 0.02$ ,  $p < 0.05$ ,  $n = 3$ ). In contrast, the ChR2 group showed decreased expression of NT-1

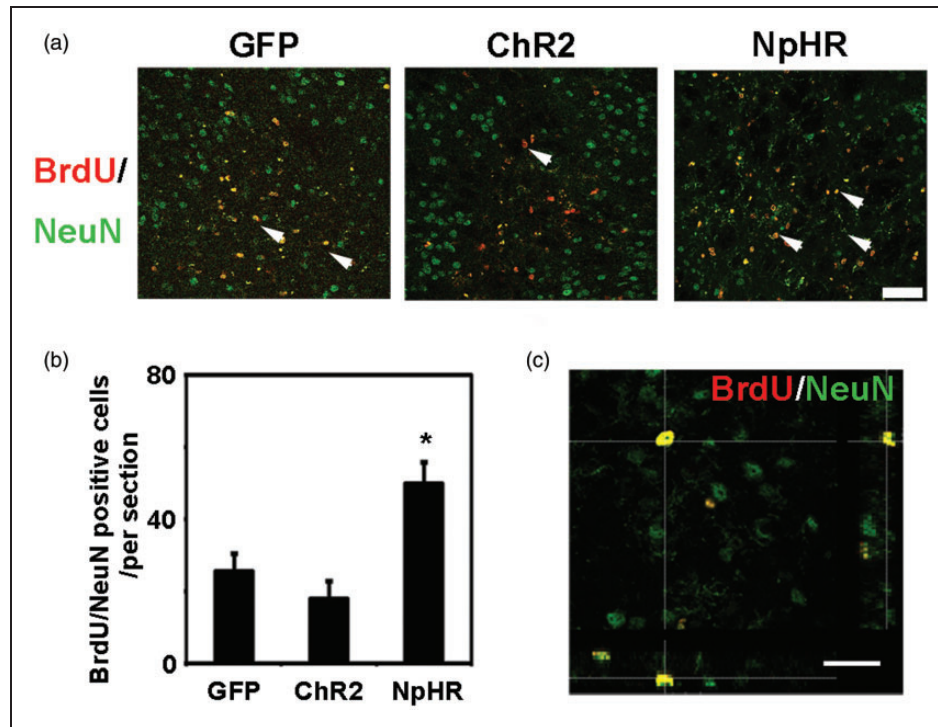


**Figure 5.** Inhibition of striatal neurons increased the number of newborn neurons in the ischemic penumbra after ischemia.

(a) BrdU/NeuN double-positive cells in the penumbra at 35 days after ischemia. Arrowheads indicate BrdU/NeuN double-positive new born neurons, bar = 50  $\mu$ m. (b) Compared to the control, mice in the inhibition group had more BrdU/NeuN double-positive newborn neurons in the penumbra at 35 days after MCAO. \* represents  $p < 0.001$ ,  $n = 6$ . (c) Three-dimensional observation of BrdU/NeuN double-positive cells in the penumbra. Bar = 30  $\mu$ m.

when compared to the control group (ChR2 =  $0.04 \pm 0.03$  vs GFP =  $0.16 \pm 0.02$ ,  $p < 0.05$ ,  $n = 3$ ). These results suggested that inhibiting but not exciting striatal neurons can increase the expression of NT-1 after ischemic stroke.

## Discussion

In the present study, we used optogenetics to specifically regulate the activity of striatal neurons and investigated the role of striatal neuronal activity in neurogenesis after ischemic stroke. We used CaMKII promoter, which is considered a forebrain-specific promoter to drive the expression of ChR2 or NpHR in striatal neurons. It is known that lentivirus containing CaMKII promoter mainly transfected excitatory neurons in the cortex and hippocampus.<sup>24</sup> Earlier study from Mayford et al.<sup>25</sup> showed that CaMKII promoter is a forebrain-specific promoter and can be used to drive the target gene expression in most striatal neurons in transgenic mice, which was further confirmed by Tsien et al.<sup>26</sup> In the research by Chuhma et al.<sup>27</sup> in 2011, using the tetracycline transactivator-tetO promoter strategy, CaMKII promoter was used to specifically drive the expression of opsins in striatal medium

spiny neuron. Consistent with these previous studies,<sup>28</sup> our results demonstrated that CaMKII promoter is able to drive ChR2 or NpHR expression in striatal neurons. In our study, opsins (ChR2 or NpHR) tagged with YFP were widely expressed and limited in the striatum at 2 weeks after injection of the lentivirus-carrying genes under the control of CaMKII- $\alpha$  (1.3KB) promoter (Figure 2(d)). In addition, we found that the majority of the YFP-positive neurons are medium spiny neurons marked by DARPP-32 (Figure 2(b) and (c)). Furthermore, in vivo electrophysiology data showed that the activity of striatal neurons transfected with ChR2 or NpHR under the control of CaMKII promoter can be successfully regulated by laser stimulation in our study.

Clinical trials have used repetitive transcranial magnetic stimulation (rTMS) or direct current stimulation to enhance neuronal activity to improve the recovery after brain ischemia.<sup>29</sup> In animal experiments, exciting cortical neurons by applying these methods or optogenetics after ischemia was shown to improve the motor performance of animals.<sup>9</sup> However, How striatal neuronal activity regulates motor function recovery remains unclear. Previous studies reported that direct current stimulation of striatal cells in chronic phase of stroke



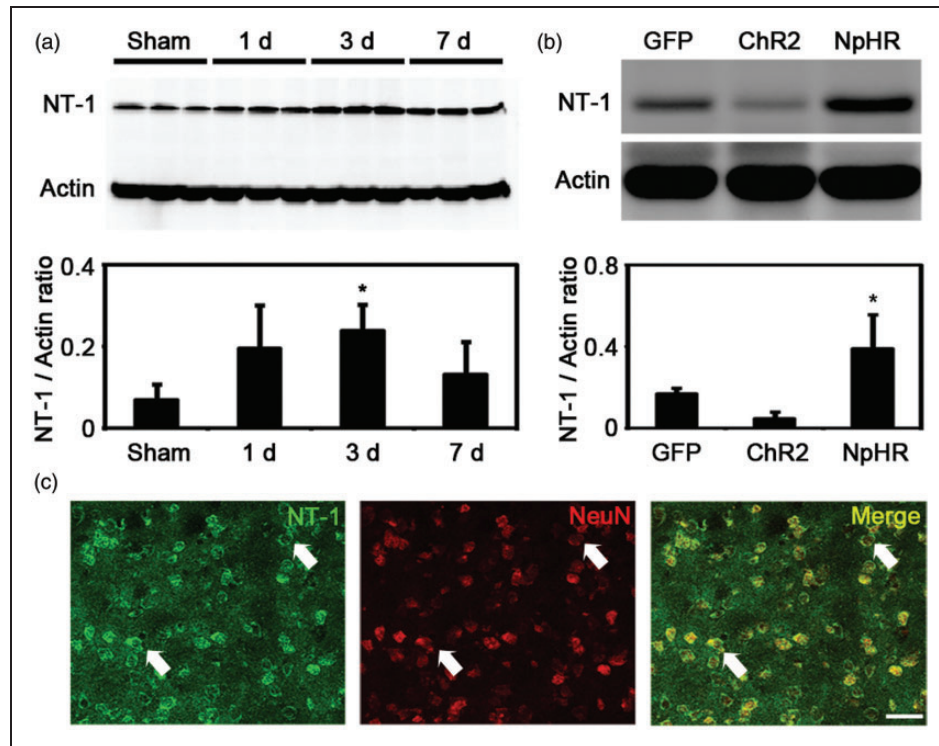


**Figure 6.** The activity of striatal neurons influenced NT-1 expression after cerebral ischemia. (a) NT-1 expression in the striatum at 1, 3 and 7 days after brain ischemia. The level of NT-1 increased significantly at 3 days after MCAO. \* represents  $p < 0.05$ ,  $n = 3$ . (b) NT-1 expression in the striatum in each group at 7 days after tMCAO. Mice in the inhibition group expressed more NT-1 compared to the control. \* represents  $p < 0.05$ ,  $n = 3$ . (c) NT-1/NeuN double positive cells in the striatum. Arrows indicates the representative neurons that express NT-1. Bar = 30  $\mu\text{m}$ .

promotes recovery.<sup>10</sup> In the present study, we found that inhibiting instead of exciting the activity of striatal neurons after ischemia improved functional outcome. This result suggests that the effects caused by optical stimulation were different from the effects caused by electrical stimulation. One possible reason is the different scope of the effective stimulated cell types. Electrical stimulation enhanced the activities of all cells around the electrode including glial cells, while optical stimulation specifically regulated the activities of target neurons.<sup>20</sup> Therefore, the downstream events, such as the secretion of neurotrophic factors, may be different between these two methods.

We found that the expression of NT-1 was increased in the NpHR group. Studies showed that NT-1 is beneficial for the recovery after cerebral ischemia.<sup>15</sup> It was also reported that injecting NT-1 protein after ischemia increased the long-term potential and inhibited neuronal apoptosis in the acute phase of ischemic stroke.<sup>18,30</sup> In the post-acute phase, Adeno Associated Virus (AAV)-mediated exogenous NT-1 overexpression in mouse brain also promoted the recovery via strengthening angiogenesis and oligodendrogenesis.<sup>16,31</sup> In addition to these functions in promoting cell maturation, NT-1 signal is also a crucial factor in

coordinating the proliferation, migration and differentiation of neural progenitor cells in the SVZ.<sup>32</sup> NT-1 was shown to promote the migration of neural progenitor cells from the SVZ after demyelination.<sup>33</sup> Thus, the increased NT-1 might contribute to the increased neurogenesis after the inhibition of striatal neuronal activity via optogenetics in our study.

In addition to NT-1, there is another possibility that could explain the functional improvements that was induced by the inhibition of striatal neuronal activity after ischemia. Medium spiny neurons (MSNs) account for more than 95% of all striatal neurons and most of them were GABAergic.<sup>27</sup> Previous studies have demonstrated that GABA is a niche signal that regulates the development of stem cells both *in vitro* and *in vivo*.<sup>34</sup> It was reported that the GABA from parvalbumin-positive neurons could limit the proliferation of NSCs in the adult mouse hippocampus.<sup>13</sup> GABA also inhibits the proliferation and migration of neural progenitor cells in the SVZ.<sup>23,35</sup> Thus, it is possible that inhibiting the activity of striatal neurons, which project dendrites and axons to the SVZ,<sup>14</sup> could decrease the secretion of GABA and promote the proliferation of NSCs in the SVZ. We found that GABA receptor inhibitor bicuculline, administrated before laser stimulation, rescued

the decrease of cell proliferation in the SVZ in the ChR2 group (Supp Figure 1). This result suggested that GABA might also play an important role in the enhancement of neurogenesis in the SVZ induced by inhibitory stimulation in the striatum.

Taken together, our present work found that optical inhibition of striatal neurons promoted neurogenesis after cerebral ischemia, which may be related with NT-1 secretion and GABA inhibition.

### Funding

The author(s) disclosed receipt of the following financial support for the research, authorship, and/or publication of this article: This study was supported by the NSFC Projects 81471178, U1232205 (GYY); 81371305 (YW; 61361160415) and 81501014 (HXS), Guangzhou Medical University project L1451012 (HXS), and the Science and Technology Commission of Shanghai Municipality project 13ZR1422600 (ZJZ).

### Acknowledgments

The authors thank Xiang Gu and Jin Xu for their technical assistance and the staffs of the Neuroscience and Neuroengineering Center for their collaborative support.

### Declaration of conflicting interests

The author(s) declared no potential conflicts of interest with respect to the research, authorship, and/or publication of this article.

### Authors' contributions

Xiaosong He, Yifan Lu: conception and design, provision of study material, collection and/or assembly of data, data analysis and interpretation, manuscript writing. Xiaojie Lin: provision of study material, collection and assembly of data. Lu Jiang, Yaohui Tang, Guanghui Tang, Xiaoyan Chen: provision of study material, collection and/or assembly of data. Zhijun Zhang, Yongting Wang, Guo-Yuan Yang: conception and design, financial support, administrative support, provision of study material, data analysis and interpretation, manuscript writing. All authors corrected and approved the manuscript.

### Supplementary material

Supplementary material for this paper can be found at <http://jcbfm.sagepub.com/content/by/supplemental-data>

### References

- Garzón-Muvdi T and Quiñones-Hinojosa A. Neural stem cell niches and homing: recruitment and integration into functional tissues. *ILAR J* 2009; 51: 3–23.
- Doetsch F, García-Verdugo JM and Alvarez-Buylla A. Cellular composition and three-dimensional organization of the subventricular germinal zone in the adult mammalian brain. *J Neurosci* 1997; 17: 5046–5061.
- Imayoshi I, Sakamoto M, Ohtsuka T, et al. Roles of continuous neurogenesis in the structural and functional integrity of the adult forebrain. *Nat Neurosci* 2008; 11: 1153–1161.
- Hou SW, Wang YQ, Xu M, et al. Functional integration of newly generated neurons into striatum after cerebral ischemia in the adult rat brain. *Stroke* 2008; 39: 2837–2844.
- Yamashita T, Ninomiya M, Hernández Acosta P, et al. Subventricular zone-derived neuroblasts migrate and differentiate into mature neurons in the post-stroke adult striatum. *J Neurosci* 2006; 26: 6627–6636.
- Burns TC, Verfaillie CM and Low WC. Stem cells for ischemic brain injury: a critical review. *J Comp Neurol* 2009; 515: 125–144.
- Murphy TH and Corbett D. Plasticity during stroke recovery: from synapse to behaviour. *Nat Rev Neurosci* 2009; 10: 861–872.
- Carmichael ST. Brain excitability in stroke: the yin and yang of stroke progression. *Arch Neurol* 2012; 69: 161–167.
- Cheng MY, Wang EH, Woodson WJ, et al. Optogenetic neuronal stimulation promotes functional recovery after stroke. *Proc Natl Acad Sci U S A* 2014; 111: 12913–12918.
- Morimoto T, Yasuhara T, Kameda M, et al. Striatal stimulation nurtures endogenous neurogenesis and angiogenesis in chronic-phase ischemic stroke rats. *Cell Transplant* 2011; 20: 1049–1064.
- Deisseroth K. Optogenetics. *Nat Meth* 2011; 8: 26–29.
- Miller G. Optogenetics. Shining new light on neural circuits. *Science* 2006; 314: 1674–1676.
- Song J, Zhong C, Bonaguidi MA, et al. Neuronal circuitry mechanism regulating adult quiescent neural stem-cell fate decision. *Nature* 2012; 489: 150–154.
- Young SZ, Lafourcade CA, Platel JC, et al. GABAergic striatal neurons project dendrites and axons into the postnatal subventricular zone leading to calcium activity. *Front Cell Neurosci* 2014; 8: 10.
- Tsuchiya A, Hayashi T, Deguchi K, et al. Expression of netrin-1 and its receptors DCC and neogenin in rat brain after ischemia. *Brain Res* 2007; 1159: 1–7.
- He X, Li Y, Lu H, et al. Netrin-1 overexpression promotes white matter repairing and remodeling after focal cerebral ischemia in mice. *J Cereb Blood Flow Metab* 2013; 33: 1921–1927.
- Sun H, Le T, Chang TT, et al. AAV-mediated netrin-1 overexpression increases peri-infarct blood vessel density and improves motor function recovery after experimental stroke. *Neurobiol Dis* 2011; 44: 73–83.
- Wu TW, Li WW and Li H. Netrin-1 attenuates ischemic stroke-induced apoptosis. *Neuroscience* 2008; 156: 475–482.
- Castillo-Paterna M, Moreno-Juan V, Filipchuk A, et al. DCC functions as an accelerator of thalamocortical axonal growth downstream of spontaneous thalamic activity. *EMBO Rep* 2015; 16: 851–862.
- Boyden ES, Zhang F, Bamberg E, et al. Millisecond-timescale, genetically targeted optical control of neural activity. *Nat Neurosci* 2005; 8: 1263–1268.
- Chen C, Lin X, Wang J, et al. Effect of HMGB1 on the paracrine action of EPC promotes post-ischemic neovascularization in mice. *Stem Cells* 2014; 32: 2679–2689.

22. Tan KR, Yvon C, Turiault M, et al. GABA neurons of the VTA drive conditioned place aversion. *Neuron* 2012; 73: 1173–1183.
23. Fernando RN, Eleuteri B, Abdelhady S, et al. Cell cycle restriction by histone H2AX limits proliferation of adult neural stem cells. *Proc Natl Acad Sci U S A* 2011; 108: 5837–5842.
24. Dittgen T, Nimmerjahn A, Komai S, et al. Lentivirus-based genetic manipulations of cortical neurons and their optical and electrophysiological monitoring in vivo. *Proc Natl Acad Sci U S A* 2004; 101: 18206–18211.
25. Mayford M, Bach ME, Huang YY, et al. Control of memory formation through regulated expression of a CaMKII transgene. *Science* 1996; 274: 1678–1683.
26. Tsien JZ, Chen DF, Gerber D, et al. Subregion- and cell type-restricted gene knockout in mouse brain. *Cell* 1996; 87: 1317–1326.
27. Chuhma N, Tanaka KF, Hen R, et al. Functional connectome of the striatal medium spiny neuron. *J Neurosci* 2011; 31: 1183–1192.
28. Tønnesen J, Parish CL, Sørensen AT, et al. Functional integration of grafted neural stem cell-derived dopaminergic neurons monitored by optogenetics in an in vitro Parkinson model. *PLoS One* 2011; 6: e17560.
29. Clarkson AN and Carmichael ST. Cortical excitability and post-stroke recovery. *Biochem Soc Trans* 2009; 37: 1412–1414.
30. Bayat M, Baluchnejadmojarad T, Roghani M, et al. Netrin-1 improves spatial memory and synaptic plasticity impairment following global ischemia in the rat. *Brain Res* 2012; 1452: 185–194.
31. Lu H, Wang Y, He X, et al. Netrin-1 hyperexpression in mouse brain promotes angiogenesis and long-term neurological recovery after transient focal ischemia. *Stroke* 2012; 43: 838–843.
32. O’Leary CJ, Bradford D, Chen M, et al. The Netrin/RGM receptor, Neogenin, controls adult neurogenesis by promoting neuroblast migration and cell cycle exit. *Stem Cells* 2015; 33: 503–514.
33. Cayre M, Courtès S, Martineau F, et al. Netrin 1 contributes to vascular remodeling in the subventricular zone and promotes progenitor emigration after demyelination. *Development* 2013; 140: 3107–3117.
34. Ge S, Pradhan DA, Ming GL, et al. GABA sets the tempo for activity-dependent adult neurogenesis. *Trends Neurosci* 2007; 30: 1–8.
35. Alfonso J, Le Magueresse C, Zuccotti A, et al. Diazepam binding inhibitor promotes progenitor proliferation in the postnatal SVZ by reducing GABA signaling. *Cell Stem Cell* 2012; 10: 76–87.